Article type : Original Research Article

Differences in White Matter Microstructure and Connectivity in Nontreatment-Seeking Individuals with Alcohol Use Disorder

Evgeny J. Chumin, B.S^{1,2}, Joaquín Goñi, PhD^{1,3,4,5}, Meredith E. Halcomb, PhD¹, Timothy C. Durazzo, PhD^{6,7}, Mario Džemidžić, PhD^{1,2,8}, Karmen K. Yoder, PhD^{1,2,9}

Department of Radiology and Imaging Sciences, Indiana University School of Medicine, Indianapolis, IN, USA.

Stark Neurosciences Research Institute, Indiana University School of Medicine, Indianapolis, IN, USA.

School of Industrial Engineering, Purdue University, West Lafayette, IN, USA.

Weldon School of Biomedical Engineering, Purdue University, West Lafayette, IN, USA.

Purdue Institute for Integrative Neuroscience, Purdue University, West Lafayette, IN, USA.

Department of Psychiatry and Behavioral Sciences, Stanford University, Stanford, CA, USA.

Department of Psychiatry, Veterans Affairs Palo Alto Health Care System, Palo Alto, CA, USA.

This is the author's manuscript of the article published in final edited form as:

Chumin, E. J., Goñi, J., Halcomb, M.E., Durazzo, T.C., Dzemidzic, M., & Yoder, K.K. (2018). Differences in White Matter Microstructure and Connectivity in Nontreatment-Seeking Individuals with Alcohol Use Disorder. Alcoholism: Clinical and Experimental Research, 0(0). https://doi.org/10.1111/acer.13629

⁸Department of Neurology, Indiana University School of Medicine, Indianapolis, IN, USA. ⁹Department of Psychology, Indiana University-Purdue University Indianapolis, Indianapolis, IN, USA.

Correspondence to: Dr. Karmen K. Yoder, Department of Radiology and Imaging Sciences, Indiana University School of Medicine, 355 West 16th Street, GH 4100, Indianapolis, IN 46202. E-mail: kkyoder@iupui.edu Phone: 317-963-7507 Fax: 317-963-7547

Supported by ABMRF/The Foundation for Alcohol Research (KKY), NIAAA 5P60AA007611-25 (pilot P50 to KKY), NIAAA R21AA016901 (KKY), NIAAA R01AA018354 (KKY), the Indiana Clinical and Translational Sciences Institute (NIH TR000006, Indiana Clinical Research Center), and NIAAA AA07462 (T32).

Abstract

Background: Diffusion weighted imaging (DWI) has been widely used to investigate the integrity of white matter (WM; indexed by fractional anisotropy, FA) in alcohol dependence and cigarette smoking. These disorders are highly comorbid, yet cigarette use has often not been adequately controlled in neuroimaging studies of alcohol dependent populations. In addition, information on white matter deficits in currently drinking, nontreatment-seeking (NTS) individuals with alcohol dependence is limited. Therefore, the aim of this work was to investigate WM microstructural integrity in alcohol use disorder by comparing matched samples of cigarette

Introduction

smoking NTS and social drinkers (SD). Methods: Thirty-eight smoking NTS and nineteen smoking SD subjects underwent DWI as well as structural magnetic resonance imaging. After an in-house preprocessing of the DWI data, FA images were analyzed with Tract-Based Spatial Statistics (TBSS). FA obtained from the TBSS skeleton was tested for correlation with recent alcohol consumption. **Results:** Smoking NTS had lower FA relative to smoking SD, predominantly in the left hemisphere (p<0.05, Family Wise Error Rate corrected across FA skeleton). Across the full sample, FA and number of drinks per week were negatively related (p=-0.348, p=0.008). Qualitative analyses of the structural connections through compromised white matter as identified by TBSS showed differential connectivity of gray matter in NTS compared to SD subjects of left frontal, temporal, and parietal regions. **Conclusions:** NTS subjects had lower white matter FA than SD, indicating compromised white matter integrity in the NTS population. The inverse relationship of entire white matter skeleton FA with selfreported alcohol consumption supports previous evidence of a continuum of detrimental effects of alcohol consumption on white matter. These results provide additional evidence that alcohol dependence is associated with reduced white matter integrity in currently drinking nontreatmentseeking alcohol dependent individuals, after controlling for the key variable of cigarette smoking. **Keywords:** alcohol use disorder, connectivity, DTI, neuroimaging, TBSS

An estimated 15 million people in the United States have an alcohol use disorder (AUD) (Department of Health and Human Sevices, 2015), which in 2010 cost the nation 249 billion dollars (Sacks et al., 2015). Additionally, in AUD, the prevalence of tobacco use has been estimated to be ~60-90%, as compared to ~10% in a light-drinking population (Falk et al., 2006, Kalman et al., 2005, Romberger and Grant, 2004). Numerous neuroimaging studies have reported deleterious effects of alcohol on regional white matter (WM) microstructure in AUD (Bagga et al., 2014, Müller-Oehring et al., 2009, Pfefferbaum et al., 2006, Pfefferbaum and

Sullivan, 2002, Pfefferbaum et al., 2000, Yeh et al., 2009, Monnig et al., 2013, Pfefferbaum et al., 2014, Segobin et al., 2015). However, this established body of research typically does not address the potential confound of cigarette smoking in abnormalities of brain structure in AUD. There is also a body of literature that indicates cigarette smoking has detrimental effects on WM (Zhang et al., 2011, Savjani et al., 2014, Baeza-Loya et al., 2016, Zou et al., 2017). However, given that up to 85% of alcoholics are also smokers (Durazzo et al., 2007b, Romberger and Grant, 2004), it is still unclear what the relative contribution of chronic alcohol misuse is to deficits in WM. Some work in nontreatment-seeking (NTS) individuals with AUD has shown differences in brain volumes of NTS compared to light drinking controls (Cardenas et al., 2005), that could be, in part, attributed to smoking status (Durazzo et al., 2007a); but the effects of extensive alcohol misuse alone have not yet been isolated. While research into WM microstructural abnormalities in detoxified/abstinent AUD is extensive,

the same cannot be said for the NTS population. This is important, as findings from detoxified alcoholics may not generalize to community-dwelling NTS. Only 8.3% of those with an AUD have sought treatment (Department of Health and Human Sevices, 2015), which makes the NTS population the majority of individuals with AUD. Additionally, as noted above, the potential influence of comorbid cigarette use in AUD has not been addressed in neuroimaging studies of the NTS population. Thus, the overarching goal of this work was to determine if there are detectable effects of alcohol dependence on WM microstructure in a currently drinking NTS population, while controlling for cigarette smoking status. Based on existing literature in detoxified AUD subjects, we hypothesized that smoking NTS will have lower WM microstructural integrity (assessed with fractional anisotropy, FA) compared to social drinking (SD) controls. To test our hypothesis, we utilized Tract-Based Spatial Statistics (TBSS) to identify areas of compromised WM microstructure in NTS. We also applied a novel, WM tractography-based

approach, to objectively identify the gray matter regions that could be targets of cortical projections that pass through any observed WM differences.

Materials and Methods

Subjects

All procedures were approved by the Indiana University Institutional Review Board in accordance with the Belmont Report. Subjects were recruited from the community using advertisements in a local paper and social media. Written informed consent was obtained after confirmation that breath alcohol concentration (BrAC) was zero in all subjects and study procedures were explained. Subjects were 21-55 years old, and able to read, understand, and complete all procedures in English. This study was a retrospective analysis of magnetic resonance imaging (MRI) data from nineteen smoking social drinkers (SD) and thirty-eight smoking nontreatment-seeking (NTS) alcohol dependent participants. MRI data were acquired in subjects who participated in the positron emission tomography (PET) studies designed to investigate the dopamine system; PET data from most subjects in the current work have been published (Albrecht et al., 2013, Yoder et al., 2011b, Oberlin et al., 2015, Yoder et al., 2016, Yoder et al., 2011a). All subjects included in the present analyses were cigarette smokers. Exclusion criteria were: history or presence of any psychiatric, neurological, or other medical disorder, current use of any psychotropic medication, positive urine pregnancy test, positive urine toxicology screen for illicit substances, and contraindications for safety in the MRI scanner. The Semi-Structured Assessment for the Genetics of Alcoholism was administered to confirm presence or absence of AUD. NTS met DSM-IV criteria for alcohol dependence, had not received treatment within the past year, and were not actively seeking treatment. The following questionnaires were also administered: a medical history and demographics questionnaire, the 90-day Timeline Follow-Back for alcohol use (TLFB), Alcohol Dependency Scale (ADS),

Fagerstrom Test for Nicotine Dependence (Pomerleau et al., 1994), Edinburgh Handedness Inventory, and an internally-developed substance use questionnaire.

Imaging

MRI imaging was done on a 3T Siemens Magnetom Trio with a 12-channel head coil array (Siemens, Erlangen, Germany). Diffusion-weighted imaging (DWI) data were acquired using monopolar Stejskal-Tanner diffusion weighting, single shell (*b*-value = 1000 s/mm²), and 48 distinct diffusion gradients (eight *b* = 0 images acquired first; GRAPPA with in-plane acceleration of 2). Echo time (TE) was 81ms, echo spacing 0.7ms, scan duration 8:10min, 128x128 matrix, anterior to posterior phase-encoding, 6/8 partial Fourier phase, 68 axial slices, and 2x2x2 mm³ isotropic voxels. There were minor variations in TE and scan duration, as the DWI sequence was incrementally adjusted over time to minimize bed vibration and image artifacts. A small subset of data (*n* = 7) were collected with one *b* = 0 volume. A high-resolution, T1-weighted, whole-brain magnetization prepared rapid gradient echo (MP-RAGE) image was acquired with the parameters optimized for the Alzheimer's Disease Neuroimaging Initiative (http://adni.loni.usc.edu/): 9:14 min, no GRAPPA, matrix size 240x256, 160 sagittal slices, 2.91ms TE, 1.05x1.05x1.2 mm³ voxels.

Image Processing

Processing was carried out with an in-house pipeline implemented in Matlab (MathWorks, version 2014b) that incorporated programs from the Oxford Centre for Functional MRI of the Brain (FMRIB) Software Library (FSL version 5.0.9)(Jenkinson et al., 2012) and Camino (Cook et al., 2006) software suites. Figure 1 illustrates the key steps of the image processing.

T1 preprocessing

Preprocessing steps included: (1) Denoising of each subjects' T1-weighted image with an optimized nonlocal means filter for 3D MRI (Coupé et al., 2008), (2) Automated cropping and

bias field correction (FSL *robustfov* and FAST), (3) Brain extraction (FSL-BET), and (4) Tissuetype (FSL-FAST) and subcortical structure (FSL-FIRST) segmentation.

Both gray and white matter (GM, WM) images from FSL-FAST were enlarged by a single modal dilation. The GM-WM spatial overlap provided an interface region that defined seed regions for tractography. A combined cerebrospinal fluid (CSF; from FSL-FAST) and subcortical GM (from FSL-FIRST) masks were used to minimize erroneous assignment of WM voxels as GM.

DWI preprocessing

Diffusion images were visually inspected for signal dropout and significant head motion artifacts. Only datasets that passed visual inspection were included. DWI images were denoised with a local principal component analysis filter (Manjón et al., 2013). The eight b = 0 volumes were spatially registered (FSL-FLIRT dof6) to the first volume and averaged to optimize image quality and minimize effects of head motion. Motion correction of each DWI volume was achieved with linear registration (FLIRT dof6) to the reference b = 0 volume. Eddy current correction was performed with FSL *eddy correct* (Jenkinson and Smith, 2001). The b = 0 volume was coregistered (dof6 and WM boundary-based registration [BBR]) to the preprocessed T1 image and this transformation was subsequently applied to the DWI data. Voxel-wise calculation of fractional anisotropy (FA) and tensor modeling were conducted using multi-tensor fitting in Camino, where each voxel was classified as either isotropic, single-tensor (anisotropic, Gaussian), or crossing fibers (anisotropic, non-Gaussian). At multiple points throughout the preprocessing steps, images were visually inspected for quality assurance.

Tract-Based Spatial Statistics (TBSS)

Voxelwise statistical analysis of the FA data was performed with FSL's Tract-Based Spatial Statistics (TBSS) (Smith et al., 2006). Each subject's FA data were aligned into a common space using the nonlinear registration (FNIRT), which uses a b-spline representation of the

registration warp field. Next, a mean FA volume was created and thinned to form an FA skeleton that represented the centers of all tracts in the sample. Each subject's aligned FA data were then projected onto the skeleton, and the resultant datasets served as input into the voxelwise statistics algorithm. Group differences were interrogated with FSL's *randomise* permutation testing. Contrasts were generated after 10,000 permutations with Threshold-Free Cluster Enhancement (TFCE) (Smith and Nichols, 2009), and were corrected for multiple comparisons (family-wise error; FWE). The anatomic locations of significant clusters were used as a starting point for post-hoc, qualitative tractography analyses (2.6). Cluster size, peak voxel significance and the corresponding coordinate, as well as the mean FA value of each significant cluster were extracted with the FSL *cluster* tool. Additionally, the mean FA value from each subject's FA skeleton was extracted using Matlab. These extracted average FA values were tested for a relationship with recent alcohol use by nonparametric regressions (Spearman's rho) in SPSS 24. Nonparametric testing was utilized because, across all subjects, recent alcohol use (drinks/week) was non-normally distributed.

Connectivity Analyses

Deterministic Tractography

Deterministic tractography conducted in Camino with the Fiber Assignment by Continuous Tracking (FACT) algorithm used a single seed per voxel at the GM-WM interface region. Fiber assignment began in a seed voxel, with 1 mm increments (1 step per voxel). Except for twotensor voxels, fiber tracking followed the major diffusion gradient from voxel-to-voxel except when the turning angle exceeded 45° in 5 steps, which resulted in termination of tracking. Encountering a two-tensor voxel led to fiber duplication, with each of the two fibers followed one of the tensor directions. Streamlines were restricted to WM voxels where FA > 0.1, and were terminated when they reached a GM voxel on either end. Very short (< 8 mm) or long (> 180 mm) streamlines were discarded.

Tract (Streamline) Isolation

To isolate fibers passing though voxels with significant group differences in FA, the TBSS output images were transformed into each subject's native space with FSL tbss_deproject. Camino *procstreamlines* projected the cluster maps onto each subject's tractography results, and constrained the tractography data to fibers that passed through the significant clusters (e.g., TBSS *p*-value volumes; Figure 1). To perform quality checks of modeled streamlines, fiber data were converted to trk format for visualization in TrackVis (Wang et al., 2007).

Gray Matter Parcellation

Each subject's gray matter was subdivided into 278 regions based on a functionally-derived parcellation (Shen et al., 2013). This allowed us to locate gray matter sources of streamlines passing through white matter areas of significantly different FA. The parcellation was applied to each subject's data by the following steps: 1) spatial transformation of the native T1 volume into MNI space (FSL: flirt-dof6, flirt-dof12, fnirt); 2) application of the individual inverse transformation parameters to the MNI template parcellation; and 3) masking the resultant native-space parcellation with each subject's GM mask from FSL-FAST. For quality assurance, the final parcellations were overlaid on the respective T1 volumes for visual inspection.

Connectivity Visualization

The number of streamlines that connected any pair of gray matter regions was obtained from a connectivity matrix generated with the Camino *conmat* function. Connections were assessed separately for NTS and SD. For each group, a region-by-region connectivity matrix was generated with the conservative requirement that, to be counted, a given connection must be present in all subjects within that group. GM regions that were connected via the significant cluster areas were visualized by an overlay of the connected GM regions for each group onto a Colin 27 (CH2) MNI brain template.

Group differences in sample characteristics were assessed with independent-samples *t*-tests or χ^2 tests (R; version 3.3.0).

Results

Subjects

Subject characteristics are presented in Table 1. NTS and SD were well-matched on all demographic characteristics and tobacco use. NTS reported significantly higher alcohol consumption and scored higher on the Alcohol Dependence Scale (ADS).

TBSS: SD vs. NTS

NTS had lower FA compared to SD, predominantly in the left hemisphere (p<0.05 TFCE, FWEcorrected; Figure 2). Thirty-three significant clusters were identified. Data for the largest (exceeding 90 mm³) and likely most relevant clusters are presented in Table 2. For a full list of clusters, the reader is referred to Supplementary Table 1.

Correlations of FA with recent alcohol use

Across all subjects, number of drinks per week had a significant negative correlation with average FA from the TBSS skeleton (Spearman's $\rho = -0.348$, p = 0.008; Figure 3).

Structural Connectivity

In SD, 42 of the 278 gray matter regions were connected though the significant clusters from the NTS < SD TBSS contrast, while NTS had 40 connected gray matter regions. Spatially, these regions were largely overlapping between groups, with some regions unique to each group. Figure 4 illustrates the connected GM regions for each group. There were qualitative differences in regional patterns of GM targets between groups (see Discussion).

This study found effects of alcohol dependence on WM microstructure in smoking nontreatmentseeking alcohol dependent individuals who had lower FA relative to smoking social drinkers. Not matching groups for smoking status is a potentially important confound that is often overlooked in neuroimaging studies of addiction. We used our results as a starting point for implementation of a novel approach to identify gray matter regions that could be the sources of denervation through the areas of compromised white matter (identified via TBSS). We also found that FA values in the whole study sample were negatively associated with recent drinking behavior.

The areas in which NTS had significantly lower FA compared to SD were primarily in the left hemisphere, notably, in the external capsule and the superior longitudinal fasciculus. FA deficits in regions that contain these tracts have been previously reported in AUD (Pfefferbaum et al., 2009, Yeh et al., 2009) and altered WM integrity in the tracts has been associated with altered cognitive function (Bagga et al., 2014, Trivedi et al., 2013). Also, detrimental effects of AUD on callosal WM have been reported to occur preferentially in the genu of the corpus callosum (Estruch et al., 1997, Pfefferbaum et al., 1996), and anterior WM tracts have also been shown to have greater deficits in FA (Pfefferbaum et al., 2009). Thus, the pattern of WM microstructural deficits that we observed in NTS are consistent with previous findings, and provide additional evidence that anterior WM and longer tracts, such as the superior longitudinal fasciculus, may be more vulnerable to the effects of alcohol. At this time, it is not clear why the results were apparently lateralized; however, it is possible that larger sample size may have revealed bilateral effects.

To begin to understand possible changes in brain function secondary to WM disruption, we employed a novel filtered tractography approach, whereupon the putative GM endpoints of compromised WM tracts were identified. There were some regional differences in the connectivity patterns between NTS and SD. Connected GM regions that were only seen in the

NTS group included areas in the frontal lobe and anterior cingulate gyrus. Connected regions that were only observed in SD included frontal lobe and middle/posterior cingulate gyrus, as well the left temporal, parietal, and occipital lobes. In NTS, the absence of connections to posterior regions in parietal and occipital lobes may be additional evidence that alcohol has detrimental effects on long WM tracts, such as the superior longitudinal fasciculus.

The observed WM deficits in NTS are likely to have functional ramifications in the brain. Recent research with functional MRI showed that functional connectivity of the cingulate cortex was associated with time to relapse in a recovering AUD sample (Zakiniaeiz et al., 2017). In addition, functional connectivity of the precuneus in response to alcohol cues was associated with severity alcohol dependence (Courtney et al., 2014). Thus, it may be the case that with continued alcohol misuse, structural differences in individuals with AUD may be related to functional deficits that alter brain function. In turn, this may contribute to the maintenance of AUD, and potentially increase the risk for relapse in those who attempt to guit drinking.

Resting state functional MRI has been used to parse the brain into networks with functional significance (Yeo et al., 2011), which assists with interpreting structural connectivity results. In the present study, regions with differential structural connectivity between NTS and SD predominantly were in the ventral and dorsal attention networks (Fox et al., 2006), frontoparietal network (Vincent et al., 2008), and the default mode network (Andrews-Hanna et al., 2010). Broadly speaking, these networks are involved in orientation of attention to internal and external stimuli, decision-making, and self-referential processes – all of which are relevant to addictive processes. Indeed, studies of AUD-related populations have reported altered function of these networks (Fryer et al., 2013, Wetherill et al., 2012, Chanraud et al., 2011). Thus, the observed structural differences in NTS in the present work are consistent with these functional findings. However, in this retrospective study, functional MRI data were not available, so we were unable to relate brain function to the observed structural differences.

There are other limitations to consider for this retrospective study. First, we were unable to test for any possible interaction of cigarette and alcohol use because a nonsmoking group was not available in this retrospective sample. We also lacked metrics on lifetime exposure to alcohol as well as continuous metrics of recent and lifetime smoking rates, which could have provided insight as to the putative cumulative effects of alcohol on WM and allowed for a more precise control for cigarette use. However, we believe that the observed negative association between recent drinking history and FA is likely related to lifetime alcohol exposure, as drinking patterns often solidify in early adulthood. Second, recent research suggests that tractography algorithms may be prone to false positive results (Maier-Hein et al., 2017). The approach we applied here was designed to reduce the likelihood of such effects via application of a conservative, deterministic tracking algorithm and by restriction of the seeding area to the GM/WM interface, rather than utilizing the full extent of all GM voxels in the brain. Finally, this approach only investigated WM connectivity through TBSS skeleton, which represents the center of core WM, and not the full extent of the WM tracts. In addition, no distinctions were made as to which specific regions were connected to one another. However, this approach provided qualitative insight into putative GM connections of compromised WM tracts in AUD. It also sets a premise for future work to investigate specific structural connectivity in AUD with regional- and/or network-based tractography approaches.

In conclusion, we used TBSS to assess the effects of alcohol dependence on WM integrity in currently-drinking subjects with alcohol dependence, while controlling for cigarette smoking status. We also found that recent drinking (a probable proxy for lifetime alcohol exposure) was inversely correlated with WM integrity. Additionally, we employed a novel, qualitative method to identify the GM regions that may be adversely affected by regions of significantly lower FA in NTS, such as the cingulate cortex and precuneus. The results strongly suggest that actively-smoking and drinking individuals with alcohol dependence have features of WM microstructural

deficits. Presence of these deficits in NTS highlights the need for additional research on consequences of alcohol misuse in currently drinking, community-dwelling AUD populations, who represent the majority of individuals with the disorder.

Acknowledgements

The authors declare no potential conflict of interests.

The authors would like to thank Dr. Daniel Albrecht, James Walters, Karen Hile, Christine Herring, Lauren Federici, Cari Cox Lehigh, and Elizabeth Patton for assistance with recruitment and data collection, as well as Michele Beal and Courtney Robbins for assistance with MR imaging. We also thank Dr. Joey Contreras for assistance with the image processing pipeline.

Authors Contribution

KKY conceptualized the study design, provided funding for the work, secured all regulatory approvals, supervised all aspects of the work, and provided intellectual input for the generation of this manuscript. EJC performed the image processing and data analyses, contributed to the computer code that facilitated processing and analyses, designed the novel qualitative approach in this work, drafted and edited the manuscript, and provided intellectual input. MD designed the MRI acquisition sequences; MD and JG drafted the computer code for processing and analyses, supervised processing and analyses, and provided intellectual input for this manuscript. TCD provided intellectual content to the data interpretation and editing of the manuscript. All authors critically reviewed the manuscript and approved the final version for publication.

- ALBRECHT, D. S., KAREKEN, D. A. & YODER, K. K. 2013. Effects of smoking on D(2)/D(3) striatal receptor availability in alcoholics and social drinkers. *Brain Imaging Behav*, 7, 326-34.
 - ANDREWS-HANNA, J. R., REIDLER, J. S., SEPULCRE, J., POULIN, R. & BUCKNER, R. L. 2010. Functional-Anatomic Fractionation of the Brain's Default Network. *Neuron*, 65, 550-562.
 - BAEZA-LOYA, S., VELASQUEZ, K. M., MOLFESE, D. L., VISWANATH, H., CURTIS, K. N.,
 THOMPSON-LAKE, D. G. Y., BALDWIN, P. R., ELLMORE, T. M., DE LA GARZA, R. &
 SALAS, R. 2016. Anterior cingulum white matter is altered in tobacco smokers. *The American Journal on Addictions*, 25, 210-214.
 - BAGGA, D., SHARMA, A., KUMARI, A., KAUR, P., BHATTACHARYA, D., GARG, M. L., KHUSHU, S. & SINGH, N. 2014. Decreased white matter integrity in fronto-occipital fasciculus bundles: relation to visual information processing in alcohol-dependent subjects. *Alcohol,* 48, 43-53.
 - CARDENAS, V. A., STUDHOLME, C., MEYERHOFF, D. J., SONG, E. & WEINER, M. W. 2005. Chronic active heavy drinking and family history of problem drinking modulate regional brain tissue volumes. *Psychiatry Research: Neuroimaging*, 138, 115-130.
- CHANRAUD, S., PITEL, A.-L., PFEFFERBAUM, A. & SULLIVAN, E. V. 2011. Disruption of Functional Connectivity of the Default-Mode Network in Alcoholism. *Cerebral Cortex,* 21, 2272-2281.
- COOK, P. A., BAI, Y., NEDJATI-GILANI, S., SEUNARINE, K. K., HALL, M. G., PARKER, G. J.
 & ALEXANDER, D. C. 2006. Camino: Open-Source Diffusion-MRI Reconstruction and Processing. 14th Scientific Meeting of the International Society for Magnetic Resonance in Medicine, p. 2759.

COUPÉ, P., YGER, P., PRIMA, S., HELLIER, P., KERVRANN, C. & BARILLOT, C. 2008. An Optimized Blockwise Nonlocal Means Denoising Filter for 3-D Magnetic Resonance Images. *Medical Imaging, IEEE Transactions on,* 27, 425-441.

- COURTNEY, K. E., GHAHREMANI, D. G., LONDON, E. D. & RAY, L. A. 2014. The association between cue-reactivity in the precuneus and level of dependence on nicotine and alcohol. *Drug and Alcohol Dependence*, 141, 21-26.
- DEPARTMENT OF HEALTH AND HUMAN SEVICES, D. 2015. National Survey on Drug Use and Health [Online]. Department of Health and Human Sevices. Available: https://www.samhsa.gov/data/sites/default/files/NSDUH-DetTabs-2015/NSDUH-DetTabs-2015/NSDUH-DetTabs-2015.htm#tab5-6a [Accessed 10 March 2017].
- DURAZZO, T. C., CARDENAS, V. A., STUDHOLME, C., WEINER, M. W. & MEYERHOFF, D. J. 2007a. Non-treatment-seeking heavy drinkers: Effects of chronic cigarette smoking on brain structure. *Drug and Alcohol Dependence*, 87, 76-82.
- DURAZZO, T. C., GAZDZINSKI, S. & MEYERHOFF, D. J. 2007b. The neurobiological and neurocognitive consequences of chronic cigarette smoking in alcohol use disorders. *Alcohol and Alcoholism,* 42, 174-185.

ESTRUCH, R., NICOLÁS, J. M., SALAMERO, M., ARAGÓN, C., SACANELLA, E., FERNÁNDEZ-SOLÁ, J. & URBANO-MÁRQUEZ, A. 1997. Atrophy of the corpus callosum in chronic alcoholism. *Journal of the Neurological Sciences*, 146, 145-151.

 FALK, D. E., YI, H.-Y. & HILLER-STURMHÖFEL, S. 2006. An epidemiologic analysis of cooccurring alcohol and tobacco use and disorders: findings from the National
 Epidemiologic Survey on Alcohol and Related Conditions. *Alcohol Research & Health: The Journal Of The National Institute On Alcohol Abuse And Alcoholism*, 29, 162-171.

FOX, M. D., CORBETTA, M., SNYDER, A. Z., VINCENT, J. L. & RAICHLE, M. E. 2006. Spontaneous neuronal activity distinguishes human dorsal and ventral attention systems. *Proceedings of the National Academy of Sciences*, 103, 10046-10051.

SHANBHAG, H., KRYSTAL, J. H. & MATHALON, D. H. 2013. Differential brain response to alcohol cue distractors across stages of alcohol dependence. *Biological Psychology*, 92, 282-291. 2012. FSL. NeuroImage, 62, 782-790. Addictions, 14, 106-123. MAIER-HEIN, K. H., NEHER, P. F., HOUDE, J.-C., CÔTÉ, M.-A., GARYFALLIDIS, E., ZHONG, J., CHAMBERLAND, M., YEH, F.-C., LIN, Y.-C., JI, Q., REDDICK, W. E., GLASS, J. O., CHEN, D. Q., FENG, Y., GAO, C., WU, Y., MA, J., RENJIE, H., LI, Q., WESTIN, C.-F., DESLAURIERS-GAUTHIER, S., GONZÁLEZ, J. O. O., PAQUETTE, M., ST-JEAN, S., GIRARD, G., RHEAULT, F., SIDHU, J., TAX, C. M. W., GUO, F., MESRI, H. Y., DÁVID, S., FROELING, M., HEEMSKERK, A. M., LEEMANS, A., BORÉ, A., PINSARD, B., BEDETTI, C., DESROSIERS, M., BRAMBATI, S., DOYON, J., SARICA, A., VASTA, R., CERASA, A., QUATTRONE, A., YEATMAN, J., KHAN, A. R., HODGES, W., ALEXANDER, S., ROMASCANO, D., BARAKOVIC, M., AURÍA, A., ESTEBAN, O.,

JENKINSON, M., BECKMANN, C. F., BEHRENS, T. E. J., WOOLRICH, M. W. & SMITH, S. M. JENKINSON, M. & SMITH, S. 2001. A global optimisation method for robust affine registration of brain images. Medical Image Analysis, 5, 143-156. KALMAN, D., MORISSETTE, S. B. & GEORGE, T. P. 2005. Co-Morbidity of Smoking in Patients with Psychiatric and Substance Use Disorders. The American Journal on

LEMKADDEM, A., THIRAN, J.-P., CETINGUL, H. E., ODRY, B. L., MAILHE, B.,

NADAR, M. S., PIZZAGALLI, F., PRASAD, G., VILLALON-REINA, J. E., GALVIS, J.,

THOMPSON, P. M., REQUEJO, F. D. S., LAGUNA, P. L., LACERDA, L. M., BARRETT,

R., DELL'ACQUA, F., CATANI, M., PETIT, L., CARUYER, E., DADUCCI, A., DYRBY, T.

B., HOLLAND-LETZ, T., HILGETAG, C. C., STIELTJES, B. & DESCOTEAUX, M. 2017.

FRYER, S. L., JORGENSEN, K. W., YETTER, E. J., DAURIGNAC, E. C., WATSON, T. D.,

The challenge of mapping the human connectome based on diffusion tractography. *Nature Communications*, 8, 1349.

- MANJÓN, J. V., COUPÉ, P., CONCHA, L., BUADES, A., COLLINS, D. L. & ROBLES, M. 2013.
 Diffusion Weighted Image Denoising Using Overcomplete Local PCA. *PLoS ONE*, 8, e73021.
- MONNIG, M. A., CAPRIHAN, A., YEO, R. A., GASPAROVIC, C., RUHL, D. A., LYSNE, P., BOGENSCHUTZ, M. P., HUTCHISON, K. E. & THOMA, R. J. 2013. Diffusion tensor imaging of white matter networks in individuals with current and remitted alcohol use disorders and comorbid conditions. *Psychology of Addictive Behaviors*, 27, 455-465.
- MÜLLER-OEHRING, E. M., SCHULTE, T., FAMA, R., PFEFFERBAUM, A. & SULLIVAN, E. V.
 2009. Global–Local Interference is Related to Callosal Compromise in Alcoholism: A
 Behavior-DTI Association Study. *Alcoholism: Clinical and Experimental Research*, 33, 477-489.
- OBERLIN, B. G., ALBRECHT, D. S., HERRING, C. M., WALTERS, J. W., HILE, K. L., KAREKEN, D. A. & YODER, K. K. 2015. Monetary discounting and ventral striatal dopamine receptor availability in nontreatment-seeking alcoholics and social drinkers. *Psychopharmacology (Berl)*, 232, 2207-16.
- PFEFFERBAUM, A., ADALSTEINSSON, E. & SULLIVAN, E. V. 2006. Supratentorial Profile of White Matter Microstructural Integrity in Recovering Alcoholic Men and Women. *Biological Psychiatry*, 59, 364-372.

PFEFFERBAUM, A., LIM, K. O., DESMOND, J. E. & SULLIVAN, E. V. 1996. Thinning of the Corpus Callosum in Older Alcoholic Men: A Magnetic Resonance Imaging Study. *Alcoholism: Clinical and Experimental Research,* 20, 752-757.

PFEFFERBAUM, A., ROSENBLOOM, M., ROHLFING, T. & SULLIVAN, E. V. 2009.

Degradation of association and projection white matter systems in alcoholism detected with quantitative fiber tracking. *Biol Psychiatry*, 65, 680-90.

PFEFFERBAUM, A., ROSENBLOOM, M. J., CHU, W., SASSOON, S. A., ROHLFING, T., POHL, K. M., ZAHR, N. M. & SULLIVAN, E. V. 2014. White matter microstructural recovery with abstinence and decline with relapse in alcohol dependence interacts with normal ageing: a controlled longitudinal DTI study. *The Lancet Psychiatry*, 1, 202-212.

- PFEFFERBAUM, A. & SULLIVAN, E. V. 2002. Microstructural but Not Macrostructural
 Disruption of White Matter in Women with Chronic Alcoholism. *NeuroImage*, 15, 708-718.
- PFEFFERBAUM, A., SULLIVAN, E. V., HEDEHUS, M., ADALSTEINSSON, E., LIM, K. O. & MOSELEY, M. 2000. In Vivo Detection and Functional Correlates of White Matter Microstructural Disruption in Chronic Alcoholism. *Alcoholism: Clinical and Experimental Research*, 24, 1214-1221.
- POMERLEAU, C. S., CARTON, S. M., LUTZKE, M. L., FLESSLAND, K. A. & POMERLEAU, O.
 F. 1994. Reliability of the fagerstrom tolerance questionnaire and the fagerstrom test for nicotine dependence. *Addictive Behaviors*, 19, 33-39.
- ROMBERGER, D. J. & GRANT, K. 2004. Alcohol consumption and smoking status: the role of smoking cessation. *Biomedicine & Pharmacotherapy*, 58, 77-83.
- SACKS, J. J., GONZALES, K. R., BOUCHERY, E. E., TOMEDI, L. E. & BREWER, R. D. 2015.
 2010 National and State Costs of Excessive Alcohol Consumption. *American Journal of Preventive Medicine*, 49, e73-e79.

SAVJANI, R. R., VELASQUEZ, K. M., THOMPSON-LAKE, D. G. Y., BALDWIN, P. R., EAGLEMAN, D. M., DE LA GARZA II, R. & SALAS, R. 2014. Characterizing white matter changes in cigarette smokers via diffusion tensor imaging. *Drug and Alcohol Dependence*, 145, 134-142.

SEGOBIN, S., RITZ, L., LANNUZEL, C., BOUDEHENT, C., VABRET, F., EUSTACHE, F., BEAUNIEUX, H. & PITEL, A.-L. 2015. Integrity of white matter microstructure in alcoholics with and without Korsakoff's syndrome. *Human Brain Mapping*, 36, 2795-2808.

- SHEN, X., TOKOGLU, F., PAPADEMETRIS, X. & CONSTABLE, R. T. 2013. Groupwise wholebrain parcellation from resting-state fMRI data for network node identification. *NeuroImage*, 82, 403-415.
- SMITH, S. M., JENKINSON, M., JOHANSEN-BERG, H., RUECKERT, D., NICHOLS, T. E.,
 MACKAY, C. E., WATKINS, K. E., CICCARELLI, O., CADER, M. Z., MATTHEWS, P. M.
 & BEHRENS, T. E. J. 2006. Tract-based spatial statistics: Voxelwise analysis of multi-subject diffusion data. *NeuroImage*, 31, 1487-1505.
- SMITH, S. M. & NICHOLS, T. E. 2009. Threshold-free cluster enhancement: Addressing problems of smoothing, threshold dependence and localisation in cluster inference. *NeuroImage*, 44, 83-98.
- TRIVEDI, R., BAGGA, D., BHATTACHARYA, D., KAUR, P., KUMAR, P., KHUSHU, S., TRIPATHI, R. P. & SINGH, N. 2013. White matter damage is associated with memory decline in chronic alcoholics: a quantitative diffusion tensor tractography study. *Behav Brain Res*, 250, 192-8.
- VINCENT, J. L., KAHN, I., SNYDER, A. Z., RAICHLE, M. E. & BUCKNER, R. L. 2008. Evidence for a Frontoparietal Control System Revealed by Intrinsic Functional Connectivity. *Journal of Neurophysiology*, 100, 3328.
- WANG, R., BENNER, T., SORENSEN, A. G. & WEDEEN, V. J. 2007. Diffusion Toolkit: A
 Software Package for Diffusion Imaging Data Processing and Tractography. *Proc. Intl.* Soc. Mag. Reson. Med., 15:3720.
- WETHERILL, R. R., BAVA, S., THOMPSON, W. K., BOUCQUEY, V., PULIDO, C., YANG, T. T.
 & TAPERT, S. F. 2012. Frontoparietal connectivity in substance-naïve youth with and without a family history of alcoholism. *Brain Research*, 1432, 66-73.

- YEH, P. H., SIMPSON, K., DURAZZO, T. C., GAZDZINSKI, S. & MEYERHOFF, D. J. 2009.
 Tract-Based Spatial Statistics (TBSS) of diffusion tensor imaging data in alcohol
 dependence: abnormalities of the motivational neurocircuitry. *Psychiatry Res*, 173, 22-30.
- YEO, B. T., KRIENEN, F. M., SEPULCRE, J., SABUNCU, M. R., LASHKARI, D.,
 HOLLINSHEAD, M., ROFFMAN, J. L., SMOLLER, J. W., ZÖLLEI, L., POLIMENI, J. R.,
 FISCHL, B., LIU, H. & BUCKNER, R. L. 2011. The organization of the human cerebral cortex estimated by intrinsic functional connectivity. *Journal of Neurophysiology*, 106, 1125-1165.
- YODER, K. K., ALBRECHT, D. S., DZEMIDZIC, M., NORMANDIN, M. D., FEDERICI, L. M., GRAVES, T., HERRING, C. M., HILE, K. L., WALTERS, J. W., LIANG, T., PLAWECKI, M. H., O'CONNOR, S. & KAREKEN, D. A. 2016. Differences in IV alcohol-induced dopamine release in the ventral striatum of social drinkers and nontreatment-seeking alcoholics. *Drug and Alcohol Dependence*, 160, 163-169.
- YODER, K. K., ALBRECHT, D. S., KAREKEN, D. A., FEDERICI, L. M., PERRY, K. M.,
 PATTON, E. A., ZHENG, Q.-H., MOCK, B. H., O'CONNOR, S. J. & HERRING, C. M.
 2011a. Reliability of striatal [11C]raclopride binding in smokers wearing transdermal
 nicotine patches. *European Journal of Nuclear Medicine and Molecular Imaging*, 39, 220-225.
- YODER, K. K., ALBRECHT, D. S., KAREKEN, D. A., FEDERICI, L. M., PERRY, K. M.,
 PATTON, E. A., ZHENG, Q. H., MOCK, B. H., O'CONNOR, S. & HERRING, C. M.
 2011b. Test-retest variability of [11C]raclopride-binding potential in nontreatment-seeking alcoholics. *Synapse*, 65, 553-61.
- ZAKINIAEIZ, Y., SCHEINOST, D., SEO, D., SINHA, R. & CONSTABLE, R. T. 2017. Cingulate cortex functional connectivity predicts future relapse in alcohol dependent individuals. *NeuroImage: Clinical*, 13, 181-187.

ZHANG, X., SALMERON, B. J., ROSS, T. J., GENG, X., YANG, Y. & STEIN, E. A. 2011.
Factors underlying prefrontal and insula structural alterations in smokers. *NeuroImage*, 54, 42-48.

ZOU, Y., MURRAY, D. E., DURAZZO, T. C., SCHMIDT, T. P., MURRAY, T. A. & MEYERHOFF,
 D. J. 2017. Effects of abstinence and chronic cigarette smoking on white matter
 microstructure in alcohol dependence: Diffusion tensor imaging at 4 T. *Drug and Alcohol Dependence*, 175, 42-50.

Figure Legends.

Figure 1. Overall processing scheme for isolating tractography-derived streamlines that passed through regions of significantly different FA in the TBSS group analyses (see text for details). Each subject's gray matter (derived by segmenting the T1 image; top left) is divided into 278 functionally-derived regions (top middle, GM regions color-coded). Diffusion-weighted image (DWI) data (bottom left) are preprocessed to obtain diffusion tensor information and fractional anisotropy (FA) volumes. Anatomical and DWI data information are combined to perform deterministic tractography (top right). FA data are analyzed with tract-based spatial statistics (TBSS). The TBSS-derived significant clusters (bottom middle; orange-red) are used to "filter" the reconstructed fiber tracts to identify those that passed through the significant clusters (bottom right). The fiber tracts are color-coded to indicate their predominant orientation (left/right in red; anterior/posterior in green; inferior/superior in blue).

Figure 2. TBSS results. Areas of significant group differences in FA (p < 0.05, *FWE*-corrected, red-yellow colors) superimposed on the mean fractional anisotropy (FA) skeleton shown in green. Smoking social drinkers (SD) compared to nontreatment seekers NTS. Axial slice

positions are illustrated in the sagittal section. For better visualization, significant voxels within the white matter skeleton were thickened with *tbss_fill*.

Figure 3. Correlation of mean FA obtained from the TBSS white matter skeleton with selfreported average number of drink per week in the past 90 days across the full sample. FA: fractional anisotropy. TFLB: Timeline Follow-Back. ρ : Spearman's rho.

Figure 4. Spatial distribution of gray matter regions connected through TBSS-derived white matter clusters that showed significant group differences in FA. Connected regions are shown for both smoking social drinkers (SD, green) and smoking nontreatment-seeking alcohol use disorder subjects (NTS; red). Note that NTS have a qualitatively distinct spatial distribution of connected GM regions that are fewer in number compared to SD. Connected gray matter regions are overlaid on a Colin 27 (CH2) MNI template brain, with MNI-coordinates provided below each slice.

Table 1. Subject Characteristics.

	SD	NTS	<i>p</i> -value	
Ν	19	38		
Age	37.8 ± 8.6	38.6 ± 8.1	n.s.	
Gender	3 F	7 F	n.s.	
Race	6 AA	17 AA	n.s.	
Ethnicity	0 HL	0 HL		
Education (years)	12.8 ± 2.3	12.7 ± 1.9	n.s.	
Handedness	19 R	36 R; 2 A		
Drinks/DD	3.4 ± 1.4	8.8 ± 3.3	< 0.05	
Drinks/Week	6.4 ± 7.5	38.4 ± 18.9		
ADS	3.9 ± 2.8	12.5 ± 5.4	< 0.05	
Fagerstrom (smokers only)	4.4 ± 1.4	4.3 ± 2.1	n.s.	

F Acce

Table 2.

Characteristics of significant clusters from the NTS < SD TBSS contrast.

		Cluster Size	FA	FA	Peak	Peak MNI
	Cluster*	(mm ³)	SD	NTS	<i>p</i> -value	coordinates [#]
					(FWE)	(mm) (x, y, z)
	1	1298	0.59 ± 0.07	0.54 ± 0.09	0.028	-39, -12, 28
	2	417	0.55 ± 0.10	0.47 ± 0.12	0.045	-31, -24, -7
	3	340	0.60 ± 0.09	0.53 ± 0.13	0.044	-19, 42, 4
	4	319	0.57 ± 0.10	0.52 ± 0.10	0.045	14, -20, 30
	5	296	0.58 ± 0.08	0.53 ± 0.09	0.045	-33, -20, -1
	6	282	0.52 ± 0.08	0.44 ± 0.07	0.044	12, 27, 14
Y	7	258	0.35 ± 0.09	0.27 ± 0.10	0.042	34, -38, 33
	8	202	0.57 ± 0.07	0.52 ± 0.10	0.044	-45, -46, 30
	9	168	0.52 ± 0.09	0.44 ± 0.08	0.046	-30, 8, 5
	10	133	0.55 ± 0.08	0.48 ± 0.08	0.048	-36, -54, 26
	11	122	0.67 ± 0.06	0.61 ± 0.08	0.046	-30, 12, 32
	12	120	0.78 ± 0.08	0.73 ± 0.09	0.042	-27, -3, 42
				1	<u> </u>	<u> </u>

Table 1.

Data are mean ± standard deviation.

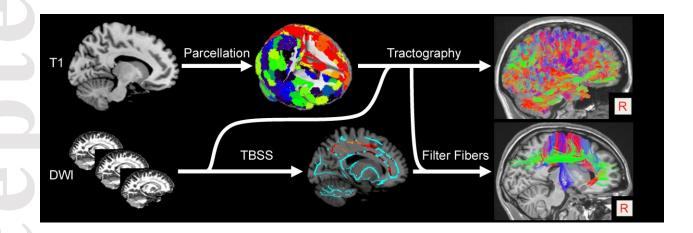
TLFB: TimeLine Follow Back. ADS: Alcohol Dependency Scale. SD: social drinkers. NTS: nontreatment-seeking alcoholics. AA: African-American. HL: Hispanic Latino. R: right. A: ambidextrous. n.s.: not significant.

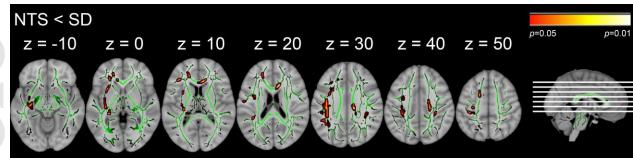
Table 2.

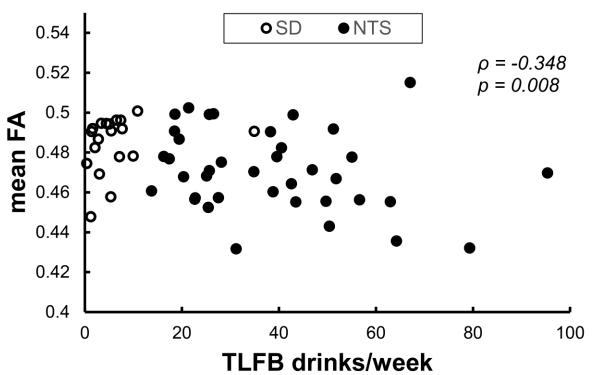
* Eleven clusters (< 90 mm³) were omitted (See Supplementary Table 1 for full list).

[#]Coordinates are in Montreal Neurological Institute (MNI) space.

TBSS: tract-based spatial statistics. SD: social drinkers. NTS: nontreatment-seekers. FA: fractional anisotropy. FWE: Family-wise error. MNI: Montreal Neurological Institute.







This article is protected by copyright. All rights reserved.

